Characterization and Optimization of a Bi-Layer BARC

Ryan M. Stamp

Abstract—**Standing wave effects have been seen throughout the history of microlithography. Due to standing wave effects, the line width control of imaged lines in photoresist is compromised. A technology that has emerged as strong solution for the reduction of standing wave effects is a Bottom Antireflective Coating (BARC) that is deposited onto the wafer before the photoresist deposition. By reducing the substrate reflectivity, the standing wave effects can also be reduced dramatically.**

The 193 nm photoresist and the bi-layer BARC films were characterized and then optimized to reduce standing wave effects within the 193 nm photoresist. A bi-layer BARC film configuration that reduces the reflectivity to less than 1% for both of the experimental numerical aperture settings of 1.05NA and 1.3NA is the goal of this project and was achieved in the RIT SMFL cleanroom. Also, a single-layer BARC system was designed to reduce substrate reflectivity to less than 1% at a setting of 1.05NA. This single-layer design was used as the control experiment or baseline to prove that a bi-layer BARC design is much more efficient than a single-layer BARC system. Simulations were conducted for the design of the multi-layer lithography systems using ILSim 1.0, an interferometric lithography simulation software as well as a simulation program on the JA Woolam Co., Inc. Variable Angle Spectroscopic Ellipsometer (VASE), which was also used to characterize the 193nm DUV resist. The simulations are run by utilizing the refractive indexes (n) and the extinction coefficients (k) of the films being used, which are the optical characteristics of the films.

Imaged lines and spaces were then exposed for each of the two designed film stacks and at the two NA settings as stated above. Imaged lines of 45 nm and 35 nm were obtained at 1.05NA and 1.3NA, respectively, for the bi-layer system, while only 45 nm lines could be obtained with the single-layer BARC system. Since the project objectives and goals were reached, a brief proposal to push the limits of the bi-layer BARC system to 1.5NA is suggested.

Index Terms—**Antireflective coatings, BARC, Immersion lithography, Standing wave effects**

This work is part of the senior design project requirement for a B.S. degree in Microelectronic Engineering at the Rochester Institute of Technology (RIT). The results of this project were presented at the 23rd Annual Microelectronic Engineering Conference on May 10, 2005 at RIT in Rochester, NY.

R. Stamp is with the Microelectronic Engineering department at the Rochester Institute of Technology in Rochester, NY.

I. INTRODUCTION

Throughout the history of semiconductor-based lithography, standing wave effects have been seen due to the high reflectivity of the silicon substrate. As the critical dimensions of IC technology become smaller and smaller, the effects of standing waves have a greater impact on sidewall angles, CD control, and exposure intensity. With the introduction of antireflective coatings, standing wave effects can be diminished by significantly reducing reflectivity within the system through absorbance or destructive interference.

A Bottom Antireflective Coating (BARC) can be either true antireflective coating, meaning the reflection from the substrate is reduced by destructive interference, or can incorporate some absorption properties that absorb the exposing light after it exits the photoresist layer. Reflection occurs at the interface between two separate media with different refractive indexes. If a light wave is traveling through a media with a small refractive index into a media with a larger refractive index, the light will reflect back at the interface between the separate media. When photoresist is deposited onto a highly reflective substrate (i.e. Silicon, nitride, silicon oxide, etc.), the interface between the two layers will cause light to be reflected back up through the photoresist resulting in constructive interference. This is the cause of the standing wave effects, which can be seen in the sidewalls of the features that are being imaged.

Figure 1 shows what negative impacts that standing wave effects can have on imaged lines and spaces. In this case, there is no BARC being used to reduce substrate reflectivity, thus the standing wave effects are very apparent. What should be 45 nm lines and spaces actually looks like ripples of exposed photoresist. This is caused solely by constructive interference which is the result of the substrate reflectivity. Again, if the constructive interference is removed from the system, then it is safe to say that the standing wave effects like the ones seen in Figure 1 would also be removed from the imaged features.

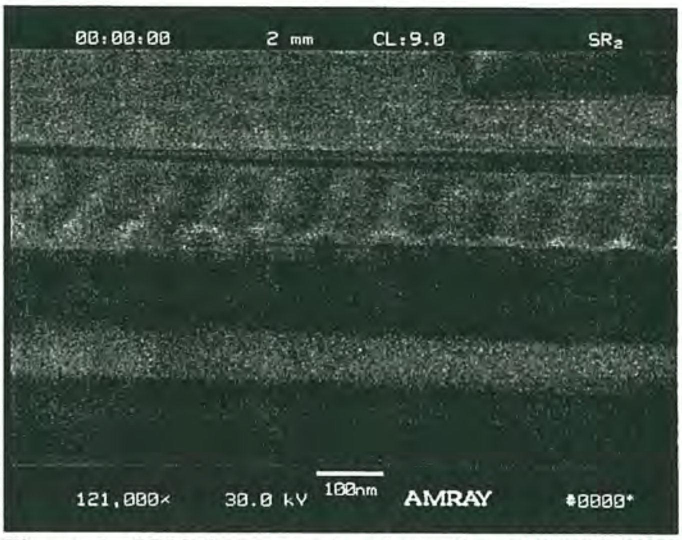

Figure 1: SEM image captured on the AMRAY SEM showing standing wave effects. This exposure was performed on the 193 nm immersion microstepper with only a single photoresist layer.

The BARC used for this project is an organic film that has absorbing properties. Therefore, the optical extinction coefficient (k) will have a profound effect on the lithography system and cannot be ignored. The complex refractive index can be represented by the following equation:

$$n^* = n + ik \tag{1}$$

where n is the real refractive index and n* is the complex refractive index. The value of k is related to absorbance and wavelength in the following equation:

$$k = \frac{\alpha\lambda}{4\pi} \tag{2}$$

where α represents the absorbance in units of μm^{-1} and λ represents the wavelength of light that is being used for the exposure. Absorbance of the light will show an exponential decay in reflectivity as the thickness of the film, may it be photoresist or BARC, increases.

In non-absorbing antireflective coatings, the refractive index of the antireflective media can be represented by the following equation:

$$n_{AR} = \sqrt{n_{SUB} \cdot n_{PR}} \tag{3}$$

where the refractive index of the antireflective coating is the square root of the product of the substrate and photoresist refractive indexes. For a dual-layer antireflective coating, like the one to be examined in this project, the following equation can be extracted from Fresnel equations:

$$\left(\frac{n_{AR2}}{n_{AR1}}\right)^2 = \frac{n_{SUB}}{n_{PR}} \tag{4}$$

The dual-film stack with refractive indexes of n_{AR1} and n_{AR2} is representing the bi-layer BARC film. This is referred to as the double-quarter, single-minimum coating, when the BARC indexes are at their minimum, the reflectance will have its broadest minimum equal to zero at a particular frequency. The film denoted by n_{AR2} should have a higher refractive index than that of the top layer, denoted by n_{AR1}. This is not relevant to the project at hand since each layer of the bi-layer BARC will have the same refractive index. Therefore, the dual-layer film must have different thicknesses in order to reduce transmission reflectivity to less than 1%. This was done within the design simulations, while including the optical extinction coefficient, and will be further discussed in the design section of the paper.

The thickness for a BARC film can be characterized by the quarter wave thickness (QWT), which is the thickness for a BARC film of a given refractive index that will induce destructive interference, hence diminishing the effects of standing waves. QWT is represented by the following equation:

$$t_{AR} = \frac{\lambda m}{4n_{AR}} \tag{5}$$

where thickness is represented by t_{AR} and the refractive index is represented by n_{AR}. Again, this instance is only relevant to the single-layer true antireflective coating. The standing waves can be reduced even more by implementing the optical extinction factor, which can be thought of as being relative to absorbance. By examining the previous equations, it can be said that the added effects of absorbance will directly benefit the cause of reducing standing waves within the lithography system.

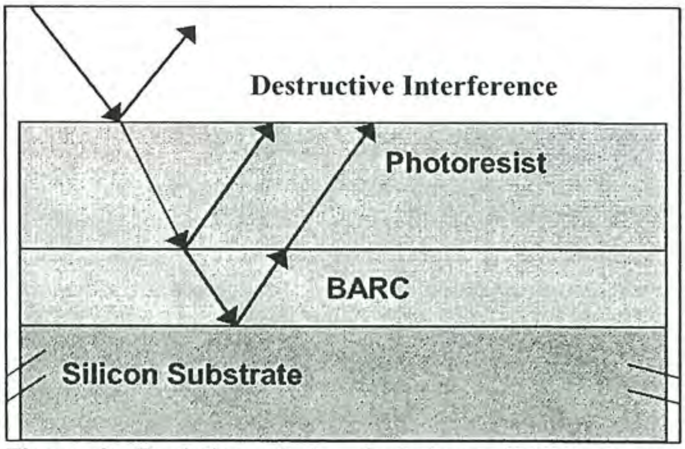

Figure 2: Depiction of the single-layer BARC theory, which uses phase shifting of the reflective light to promote destructive interference along with absorbing properties to reduce substrate reflectivity.

For any multi-layer lithography system, the Fresnel equations need to be used in order to calculate the reflection seen at each interface between two films. In the single-layer design, which is depicted by Figure 2, a phase shift of π, or 180°, is needed from the BARC to induce the destructive interference which in turn reduces standing wave effects. The Fresnel equations used for this particular single-layer BARC case are as shown:

$$R = \left(\frac{n_{PR} - n_{BARC}}{n_{PR} + n_{BARC}} \right)^2$$

(6)

$$R = \left(\frac{n_{BARC} - n_{SUB}}{n_{BARC} + n_{SUB}} \right)^2 . \quad (7)$$

These two reflection equations are the only equations of interest, since the reflections of the photoresist/BARC interface and the BARC/substrate interface will actually be used. The interface between the highly pure water ambient and the photoresist is not of a concern because there is no reflection from this interface that enters the photoresist film. Note that there is only the refractive index of the films that are a concern in this model.

In turn, Equations 3-7 are only valid calculation techniques if the exposing light is at normal incidence, meaning a 0° incident angle. These equations are then only valid when exploring small NA applications, as opposed to the hyper-NA applications with which this project is concerned with. The simulation software used for the simulation do use calculation based off of standard thin film calculation techniques.

As previously stated, absorption is a factor that is very prominent in organic BARCs and resists. The transmission within a layer can be exponentially related to the absorption of radiation (α) and the thickness of the single-layer BARC film by the following equation:

$$T = e^{-2 \cdot \alpha \cdot t_{BARC}} \quad (8)$$

where T is the transmission, t_{BARC} is the thickness of the BARC, and α is the absorption in units of μm^{-1}. Equation 8 is closely related to Equation 2, which shows exactly how absorption of radiation correlates to the optical extinction coefficient. While keeping the absorption properties of the BARC film, it can be deduced from Equation 8 that an increase in BARC thickness will increase the exponential decay of reflection within the lithography system.

By using all of the previously discussed information, bi-layer BARC configurations have a few more advantages over single-layer BARC systems. In a dual-layer design, the lower BARC film should have a relatively high optical extinction coefficient, which will cause the lower BARC to absorb as much incident radiation as possible before the radiation reaches the highly reflective substrate. By having the upper BARC refractive index matching up to the refractive index of the photoresist, in theory, there is no reflection between the two media, as shown in Equation 6 and Equation 7. By using both of these concepts, it is possible to reduce reflection over a wide range of incident angles upon exposure.

II. Design

A. Materials

Since immersion lithography is being utilized for this experiment, there are a couple more materials needed other than the photoresist and the bi-layer BARC stack. Ultra-pure H_2O is used for the ambient on the immersion microstepper and has a refractive index of 1.437 with an optical extinction coefficient that is insignificant compared to the rest of the films used. Also, the top-coat helps protect the photoresist from basic contamination from the surrounding environment, which can also be detrimental to the photoresist.

The photoresist itself is a TOK 193 nm DUV Photoresist that has an n value of 1.71 and a k value of 0.039. Next, the upper BARC film used is from AZ Electronic Materials. This BARC is actually a 248 nm BARC, but it contains the necessary optical characteristics for this experiment. The n and k values of the upper BARC are 1.7 and 0.11, respectively. Notice that the refractive index of the photoresist matches up almost exact with the upper BARC. As stated in the introduction, this match of refractive indexes can significantly reduce the reflection at the photoresist/Upper BARC interface. The lower BARC is made by Brewer Science and has an n value of 1.82 and a k value of 0.34. Both characteristic values are much higher than the upper BARC. Again, this is to ensure that the incident radiation that makes it down to the substrate is reduced as much as possible to prevent a high substrate reflectivity. This lower BARC is also used as the BARC for the single-layer BARC design.

B. Simulation

As stated in the abstract, the simulations were performed using ILSim 1.0 and the simulation software package provided by JD Woolam Co., Inc. For both the single-layer and the bi-layer BARC designs, a photoresist thickness of 170 nm was chosen. This is an extremely thick photoresist for this type of processing, since the aspect ratio for each case may be 4:1 or even 5:1. The simulations were then run many times to find the optimal thickness for the single-layer BARC and the bi-layer BARC. After a few iterations, the best thicknesses for the given materials were found.

For the single-layer BARC design, the optimal BARC thickness was seen to be 39 nm at the 1.05NA. The substrate reflectivity was seen to be much smaller than the desired 1%. This same thickness was used for the lower BARC layer of the bi-layer BARC design for simplicity. After many more iterations of the simulation software, the optimal upper BARC thickness was found to be 59 nm, which happened to be the thinnest that this particular BARC from AZ Electronic

Materials could be spin-coated. As seen in Figure 3, the bi-layer BARC design provides a wide range of incident exposure angles with reflectivity less than 1% that cannot be obtained by a single-layer BARC stack. The incident angles of interest are from 38° to 50°, which can be directly related to the numerical aperture setting in the following equation:

$$NA = n_{PR} \cdot \sin \theta_i \qquad (9)$$

where n_{PR} is the refractive index of the photoresist and θ_i is the incident angle of exposure. By examining Figure 3, it is safe to say that the bi-layer BARC stack can reduce reflectivity to less than 1% for an even wider range than it was designed.

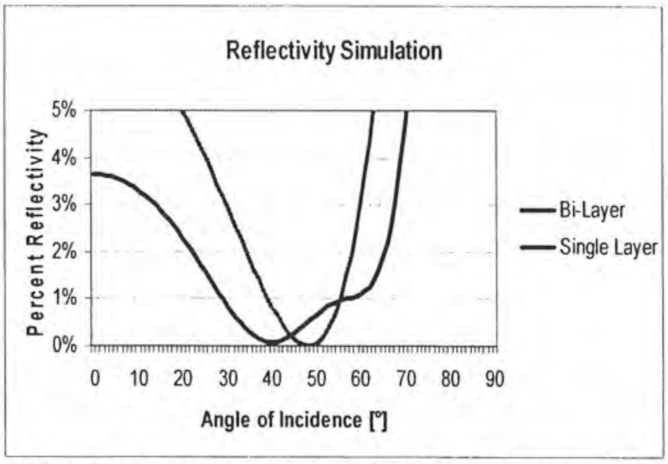

Figure 3: Simulation results of the bi-layer BARC and single-layer BARC designs.

III. PROCESSING

The processing required for this project is not extensive by any means, so a brief overview should be sufficient. As stated earlier, a top-coat was used as protection from contaminants that could jeopardize some of the optical properties needed from the resist. The top-coat is also used for a development technique that actually develops from the side. The top-coat assists the imaged lines and spaces with support since the aspect ratio of the resist would normally cause the imaged lines to collapse. A case where a top-coat was not used at a 1.3NA exposure setting can be seen in Figure 4. By developing from the side, it is feasible to be able to view visible lines and spaces clearly on the AMRAY 1830 SEM.

The exposures were completed on the 193 nm ArF immersion microstepper for the 1.05NA exposures and then on the work bench for the 1.3NA exposures. The mask used has simple lines and spaces at a pitch of 600 nm, which is greatly reduced from the high-NA exposures performed for this experiment. Only parts of the wafers were used for each exposure test. After exposure and the post exposure bake (PEB), the wafers are split across the exposure area, perpendicular to the imaged lines. The sample is then developed from the side using 1:10 CD-26 developer for 30 seconds. The sample is then coated with gold to prevent charging of the photoresist from the SEM that would damage the sample. Erect imaged lines were captured on the AMRAY 1830 SEM and can be seen in the results section of this paper.

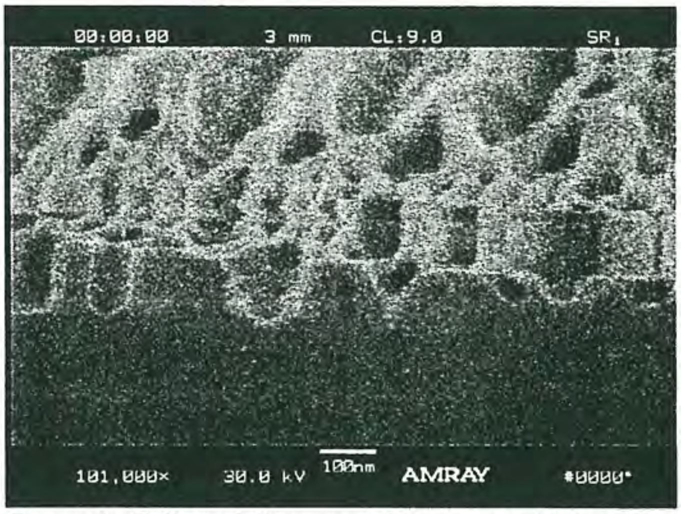

Figure 4: Collapsed lines caused by a very high aspect ratio. This bi-layer sample was exposed with an NA of 1.3.

IV. RESULTS

As previously stated in the abstract, lines and spaces of a 90 nm pitch and a 70 nm pitch were imaged in the 170 nm TOK photoresist using the optimized bi-layer BARC design. The single-layer design did produce lines and spaces with a 90 nm pitch at the 1.05NA setting, but no lines were imaged at the 1.3NA setting. Lines and spaces at a 90 nm pitch are shown in Figure 5 for the single-layer BARC and in Figure 6 for the bi-layer design.

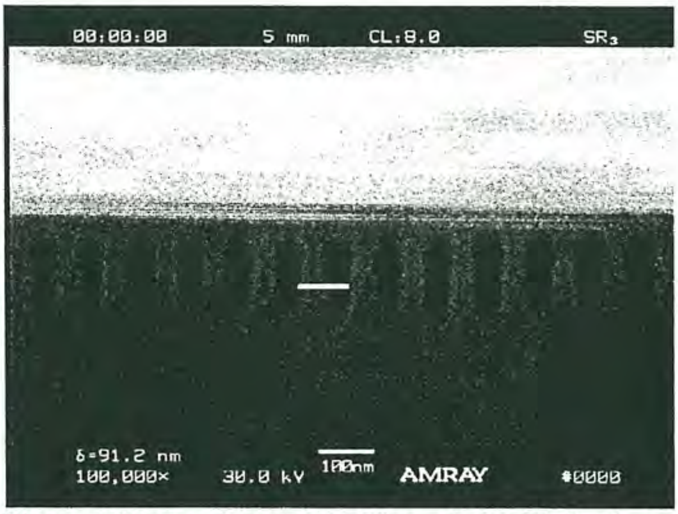

Figure 5: Lines and spaces of a 90 nm pitch with the single-layer BARC design at 1.05NA.

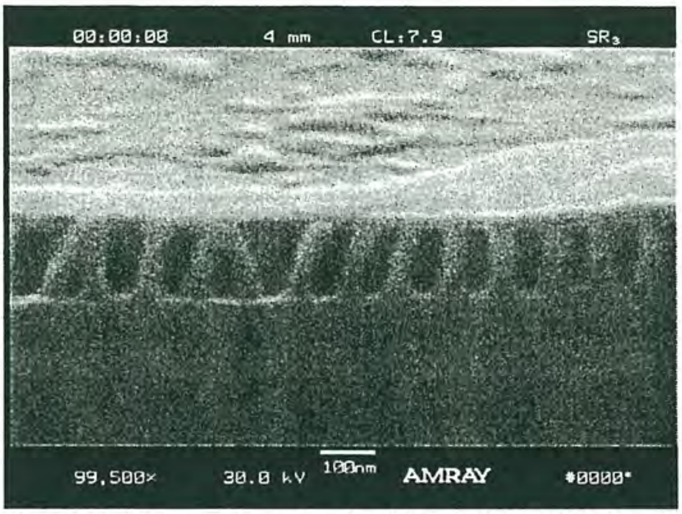

Figure 6: Lines and spaces of a 90 nm pitch with the bi-layer BARC design at 1.05NA. Some of the collapsing effects from the high aspect ratio can be seen.

The bi-layer BARC proved to work very well at the 1.3NA setting and produced imaged lines and spaces at a pitch of 70 nm, as seen in Figure 7.

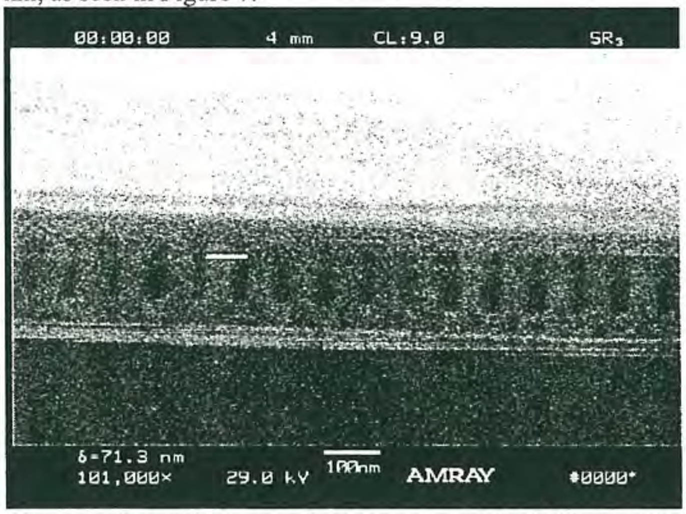

Figure 7: Imaged lines and spaces at a pitch of 70 nm. The sample was exposed at an NA setting of 1.3NA utilizing the bi-layer BARC design.

V. Conclusion

A bi-layer BARC system was designed for use with the 193 nm immersion lithography system at RIT. The bi-layer BARC design was simulated to find optimal thicknesses for each thin film, and then replicated in the SMFL cleanroom. The bi-layer BARC design was able to image lines and spaces of a 90 nm pitch and a 70 nm pitch at an 1.05NA setting and a 1.3NA setting, respectively. Verification of the imaged lines and spaces without any apparent standing wave effects was done by capturing images on the AMRAY 1830 SEM.

In future work, other multi-layer BARC stacks should be designed to widen the range of incident angles that the BARC can ensure less than 1% reflection off of the substrate with the use of a full design of experiments (DOE). This can be done with three or even more layers of BARC, or just by finding different materials with optical characteristics that may be suitable for this goal.

Acknowledgment

The author would like to give a special thanks to Yongfa Fan who made himself available as much as needed. The author would like to also thank Rohm & Haas, AZ Electronic Materials, Brewer Science, and TOK for the use of their development materials and, also, to Lambda Physik for the 193nm laser which was used for exposures. Finally, the author would like to thank Dr. Bruce Smith, the acting advisor for this project.

References

[1] B.W. Smith, L. Zavyalova, A. Estroff, "Benefiting from polarization – effects of high-NA on imaging," *Proc. SPIE 5377*, (2004).
[2] ILSim 1.0 was developed By Yongfa Fan
[3] J.R. Sheats, B.W. Smith, "Microlithography – Science and Technology," *Marcel Dekker*, (1998)
[4] D. J. Abdallah, M. Neisser, *et al*, "193nm dual layer organic B.A.R.C.s for high NA immersion lithography," *AZ® Electronic Materials* (2005)

Ryan M. Stamp is originally from Buffalo, New York and earned a B.S. in Microelectronic Engineering from the Rochester Institute of Technology in 2005. He has worked for Micron Technologies (Manassas, VA) on co-op assignments, accumulating a year of co-op experience. He will be working fulltime back at Micron Technologies in the 300 mm CVD department in early September 2005.